Synaptotagmin I functions as a calcium regulator of release probability

Rafael Fernández-Chacón*†‡, Andreas Königstorfer‡§, Stefan H. Gerber*, Jesús García‖, Maria F. Matos*, Charles F. Stevens¶, Nils Brose§, Josep Rizo‖, Christian Rosenmund† & Thomas C. Südhof*

** Center for Basic Neuroscience, Department of Molecular Genetics, and Howard Hughes Medical Institute, The University of Texas Southwestern Medical Center, Dallas, Texas 75390-9111, USA*
§ Max-Planck-Institut für experimentelle Medizin, and † Max-Planck-Institut für biophysikalische Chemie, 37070 Göttingen, Germany
‖ Departments of Biochemistry and Pharmacology, The University of Texas Southwestern Medical Center, Dallas, Texas 75390, USA
¶ The Salk Institute, and Howard Hughes Medical Institute, La Jolla, California 92037, USA
‡ These authors contributed equally to this work

In all synapses, Ca^{2+} triggers neurotransmitter release to initiate signal transmission. Ca^{2+} presumably acts by activating synaptic Ca^{2+} sensors, but the nature of these sensors—which are the gatekeepers to neurotransmission—remains unclear. One of the candidate Ca^{2+} sensors in release is the synaptic Ca^{2+}-binding protein synaptotagmin I. Here we have studied a point mutation in synaptotagmin I that causes a twofold decrease in overall Ca^{2+} affinity without inducing structural or conformational changes. When introduced by homologous recombination into the endogenous *synaptotagmin I* gene in mice, this point mutation decreases the Ca^{2+} sensitivity of neurotransmitter release twofold, but does not alter spontaneous release or the size of the readily releasable pool of neurotransmitters. Therefore, Ca^{2+} binding to synaptotagmin I participates in triggering neurotransmitter release at the synapse.

Neurotransmitter release is triggered rapidly by Ca^{2+} (in less than 1 ms)[1–3], but it is unknown how Ca^{2+} acts, and the identity of the Ca^{2+} sensor(s) involved is controversial[4–7]. One of the candidates for a Ca^{2+} sensor in release is synaptotagmin I, a synaptic vesicle protein that is selectively required for fast Ca^{2+}-dependent release[8,9]. Synaptotagmin I contains two C_2 domains (the C_2A and C_2B domains), which are composed of eight-stranded β-sandwiches, with three flexible loops emerging on top and four at the bottom[10–13]. Both C_2 domains bind several Ca^{2+} ions exclusively through their top loops, but only Ca^{2+} binding to the C_2A domain has been studied in detail[12,13]. The C_2A domain ligates three Ca^{2+} ions in incomplete coordination spheres formed primarily by aspartate residues in the top loops (Fig. 1).

The intrinsic Ca^{2+} affinity of the C_2A domain is low, probably because of the incomplete coordination spheres. Phospholipid membranes increase the overall Ca^{2+} affinity of the C_2A domain up to 5,000-fold (dissociation constant, $K_d \approx 10\ \mu M$)[14,15]. Native full-length synaptotagmin I also exhibits a low intrinsic Ca^{2+}-binding affinity that is increased markedly by phospholipid membranes[16]. Phospholipid membranes probably enhance Ca^{2+} binding to synaptotagmin I by providing additional ligands for Ca^{2+} in the incomplete coordination spheres of the Ca^{2+}-binding sites[15], as was also observed for the C_2 domain of protein kinase C (PKC)[17,18]. Thus, in the presence of Ca^{2+} and phospholipids, the C_2A domain forms a ternary complex in which Ca^{2+} is simultaneously ligated by the top loops of the C_2A domain and by phospholipid headgroups, and the phospholipids are bound by the Ca^{2+} ions and by positively charged residues that surround the Ca^{2+}-binding sites in the C_2A domain (Fig. 1).

In addition to phospholipid membranes, synaptotagmin I binds to syntaxin as a function of Ca^{2+}, although higher Ca^{2+} concentrations are required[19–21]. At least at some synapses, release is activated at ~10 μM free Ca^{2+} (refs 22–24), indicating that the exocytotic Ca^{2+} sensor has a substantially higher affinity than previously thought. The Ca^{2+} affinity corresponds well to the Ca^{2+} affinity of synaptotagmin I in the presence of phospholipids, suggesting that Ca^{2+} binding to synaptotagmin I may regulate exocytosis *in vivo*. However, confirming this function has proved technically daunting. Simply mutating Ca^{2+}-coordinating residues in a single C_2 domain of synaptotagmin I is not effective because other Ca^{2+}-binding sites remain[12,15], and because interactions between the two C_2 domains[25] might provide additional coordination sites for Ca^{2+}. Furthermore, extensive mutations to completely abolish Ca^{2+} binding may cause unintended effects, such as mistargeting, destabilization or misfolding.

To circumvent these problems, here we have pursued an alternative approach, and studied a point mutation in synaptotagmin I that changes the Ca^{2+}-binding affinity of synaptotagmin I without affecting its three-dimensional structure. We have correlated the change in Ca^{2+} binding with the physiological consequences of the same mutation after it was introduced into the endogenous

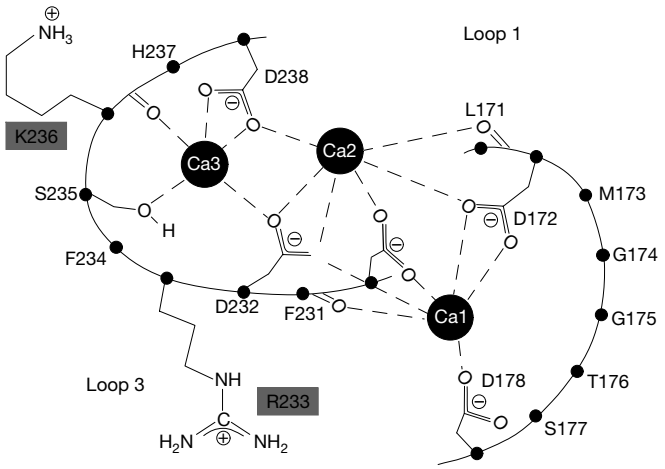

Figure 1 Architecture of the Ca^{2+}-binding sites at the top of the C_2A domain of synaptotagmin I. The three Ca^{2+}-binding sites are formed by two loops 1 and 3 at the top of the C_2A domain. Five aspartate residues, one serine residue, and two backbone carbonyl groups coordinate the three bound Ca^{2+} ions, which are labelled Ca1, Ca2 and Ca3. Arginine 233 (R233) and lysine 236 (K236), positively charged residues that surround the Ca^{2+}-binding sites and that were mutated in this study, are highlighted by a grey box. Residues are shown in single-letter amino acid code, and are identified by number (adapted from ref. 12).

synaptotagmin I gene in mice. Our results show that a mutation in synaptotagmin I that selectively decreases its apparent Ca^{2+} affinity by a factor of two causes a corresponding decrease in the Ca^{2+} sensitivity of neurotransmitter release, suggesting that Ca^{2+} binding to synaptotagmin I directly determines Ca^{2+} triggering of exocytosis.

A mutant synaptotagmin I with reduced Ca^{2+} affinity

Previous results suggested that mutations in the positively charged residues surrounding the Ca^{2+}-binding sites of the C_2A domain of synaptotagmin I influence Ca^{2+} binding[15,26]. We therefore characterized mutations in two of these positively charged residues, R233Q and K236Q (Fig. 1), by NMR spectroscopy of the purified C_2A domains with and without Ca^{2+}. Comparison of their Ca^{2+}-free $^1H-^{15}N$ heteronuclear single-quantum correlation (HSQC) spectra (Fig. 2a–c, red contours) showed that the mutations caused little perturbation in the spectra, and thus had no significant effect on the three-dimensional structure of the domain. This is not unexpected as the R233 and K236 side chains are freely exposed on the surface of the C_2A domain[11], and each mutation only neutralizes one of four basic residues surrounding the Ca^{2+}-binding sites (Fig. 1).

We next examined the intrinsic Ca^{2+}-binding properties of the mutants using Ca^{2+} titrations monitored with $^1H-^{15}N$ HSQC spectra (Fig. 2a–c, black contours). We used Ca^{2+}-induced chemical-shift changes of cross-peaks from residues close to the Ca^{2+}-binding sites as indicators of Ca^{2+} binding. The sequential coordination of the three Ca^{2+} ions is manifested by three components in the Ca^{2+}-dependent chemical-shift changes (for example, the cross-peak of S235 HN; Fig. 2d–f, blue contours)[12]. The affinities of the different Ca^{2+}-binding sites were determined from plots of the Ca^{2+}-dependent changes in chemical shifts that are strongly affected by Ca^{2+} binding to a particular Ca^{2+}-binding site. Thus, the ^{15}N chemical shift of the K200 HN cross-peak is primarily affected by Ca^{2+} binding to site Ca1 (Fig. 2a–c, arrow), and the ^1H chemical shift of the S235 HN cross-peak by Ca^{2+} binding to site Ca2 (Fig. 2d–f). Although the S235 side chain coordinates the Ca^{2+} ion in site Ca3, the S235 HN cross-peak is strongly influenced by Ca^{2+} binding to Ca2 because the peptide backbone of S235 is very close to this site[12].

In the wild-type C_2A domain, our Ca^{2+} titrations confirmed previous estimates[12,13] of the intrinsic Ca^{2+} affinities for Ca1 (K_d = 54 μM Ca^{2+}) and Ca2 (K_d = 530 μM Ca^{2+}). We could not saturate binding to Ca3 even at 40 mM Ca^{2+}, indicating a K_d of more than 20 mM. The R233Q and K236Q mutants retained Ca^{2+} binding to all three sites, as expected from the lack of a structural change; however, the R233Q mutant exhibited a selectively higher Ca^{2+} affinity at site Ca1 with a K_d of 27 μM (Fig. 2), whereas sites Ca2 (K_d = 420 μM) and Ca3 ($K_d > 20$ mM) behaved similarly to those of the wild type (Table 1). The selectively lower K_d for Ca1 in the R233Q mutant was confirmed in independent titrations with a lower protein concentration (data not shown).

The K236Q mutant of the C_2A domain exhibited Ca^{2+} affinities similar to the wild-type domain ($K_d \approx 51$ μM and $K_d \approx 530$ μM Ca^{2+} for Ca1 and Ca2, respectively). Ca3 may have a slightly higher affinity in the K236Q mutant, but Ca^{2+} binding to this site could not be saturated, preventing a quantitative comparison. Thus, two substitutions in positively charged residues close to the Ca^{2+}-binding sites, R233Q and K236Q, had no effect on the three-dimensional structure of the C_2A domain, but the R233Q substitution caused a selective increase in the intrinsic Ca^{2+} affinity of site Ca1, whereas the K236Q mutant did not.

R233Q decreases the overall Ca^{2+} affinity of the C_2A domain

Phospholipid membranes are thought to increase the Ca^{2+} affinity of synaptotagmin I by providing additional coordination sites for Ca^{2+} in the C_2A domain, and possibly also in the C_2B domain[10–16]. As a result, the overall Ca^{2+} affinity of synaptotagmin I, defined here as the Ca^{2+} affinity in the presence of phospholipid membranes, is determined by formation of the entire C_2 domain/Ca^{2+}/phospholipid complex. Thus, changes in the intrinsic Ca^{2+} affinity of a C_2 domain, such as the increased affinity for Ca1 in the R233Q mutant, may not necessarily translate into similar changes in overall Ca^{2+} affinity. We therefore measured the overall Ca^{2+} affinity of R233Q and K236Q mutant and wild-type C_2A domains using Ca^{2+}-dependent phospholipid binding as an assay with liposomes comprising 30% phosphatidylserine and 70% phosphatidylcholine (Fig. 3). As judged by this assay, the R233Q mutation caused a

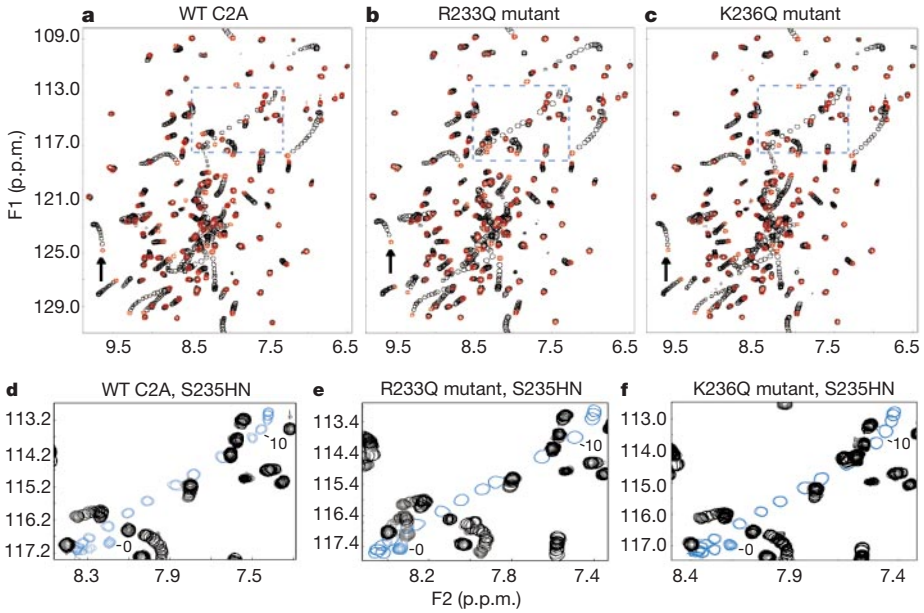

Figure 2 Ca^{2+} titrations of wild-type and mutant C_2A domains monitored by $^1H-^{15}N$ HSQC spectra. **a–c**, Superposition of $^1H-^{15}N$ HSQC spectra acquired at 0–40 mM Ca^{2+} concentrations. Spectra recorded in the absence of Ca^{2+} are shown in red, and spectra obtained at the various Ca^{2+} concentrations in black. Dashed boxes highlight the locations of the expansions shown in **d–f**; blue arrows identify the positions of the K200 HN cross-peak. **d–f**, Expansions of the $^1H-^{15}N$ HSQC spectra shown in **a–c** to illustrate the changes in the S235 HN cross-peak (blue contours) induced by Ca^{2+}. All other cross-peaks are shown in black. Note that titration of the S235 backbone cross-peaks (S235 HN) exhibits the largest changes on Ca^{2+} binding to site Ca2 because of the proximity of the S235 HN group to this site.

twofold decrease in overall Ca^{2+} affinity, in spite of an increase in intrinsic Ca^{2+} affinity. By contrast, the K236Q mutation had no effect on overall Ca^{2+} affinity similar to its lack of an effect on intrinsic Ca^{2+} affinity.

Formation of the C_2A domain/Ca^{2+}/phospholipid complex should depend on the phospholipid composition, and thus the overall Ca^{2+} affinity should also be sensitive to phospholipid composition. To test this, we measured the Ca^{2+} affinity of wild-type and R233Q mutant C_2A domains with membranes containing 22.5%, 30% or 45% phosphatidylserine. As predicted, the overall Ca^{2+} affinity of the wild-type C_2A domain strongly depended on the density of negative charges on the liposome surface (Table 1). The Ca^{2+} affinity of the R233Q mutant was roughly twofold lower than that of the wild-type C_2A domain with 22.5 and 30% phosphatidylserine, plausible concentrations of negatively charged phospholipids as compared with physiological membranes. An even larger decrease in Ca^{2+} affinity was observed with 45% phosphatidylserine (Table 1).

The Ca^{2+} affinity of the C_2A domain was independent of the density of recombinant protein on the glutathione beads used in the assay because a threefold variation of this density had no effect on apparent Ca^{2+} affinity (Table 1). These results suggest that although the intrinsic Ca^{2+} affinity is enhanced in the R233Q mutant (Fig. 2), its overall Ca^{2+} affinity is depressed because phospholipids are less able to bind to the Ca^{2+}/C_2A domain complex. Surprisingly, the K236Q mutation does not have the same effect on Ca^{2+} binding as the R233Q mutation, although it is located next to R233 close to the Ca^{2+}-binding sites. This suggests that it is not the proximity of a positively charged residue to the Ca^{2+}-binding sites, but the precise location of this charge, that is critical in determining the Ca^{2+} affinity.

Generation of mice with point mutations in synaptotagmin I

We isolated a mouse genomic clone that includes a single exon encoding residues 214 to 269 of synaptotagmin I, and used this to construct three targeting vectors with the same overall design (Fig. 4)[27]. A *neomycin* resistance gene was placed into the intron next to the exon for positive selection, and was flanked by a short arm with the exon on one side, and a long arm with intron sequences on the other side. In addition, two copies of the thymidine kinase gene were situated at the end of the short arm for negative selection (Fig. 4). The three targeting vectors differed only in the sequence of the exon which included either the R233Q substitution, the K236Q substitution, or no substitution (to generate wild-type control mice with the same *neomycin* resistance gene in the intron). The three vectors were used for homologous recombination in embryonic stem cells, yielding mutant cell clones that were injected into blastocysts to obtain 'knockin' mice.

We produced three knockin mouse lines. All lines contain a *neomycin* resistance gene in the intron, but differ in the sequences of the adjacent exon which is either wild type or includes the R233Q or K236Q substitution. By crossing R233Q knockin and K236Q knockin mice with wild-type knockin mice, we obtained double heterozygous mice with precisely controlled genetic backgrounds. The double heterozygotes were bred to each other, resulting in homozygous wild-type or mutant knockin littermates with identical intron sequences. Both types of homozygous mutant knockin mice were viable and fertile, and exhibited no obvious morbidity. Synaptotagmin I was fully expressed in all three knockin mouse lines, indicating that the inserted *neomycin* resistance gene in the intron did not alter transcription of synaptotagmin I, and that the mutations introduced in the C_2A domain did not produce unstable or mistargeted synaptotagmin I protein (Fig. 4).

Ca^{2+} affinity of native wild-type and mutant synaptotagmin I

To confirm that the R233Q substitution affects Ca^{2+} binding to native brain synaptotagmin I and not only to the isolated C_2A domain, we examined the Ca^{2+}-dependent phospholipid- and syntaxin-binding properties of native wild-type and R233Q mutant synaptotagmin I. Full-length synaptotagmin I is prone to nonspecific interactions, presumably because its amino-terminal transmembrane region is highly palmitoylated and indiscriminately binds to hydrophobic surfaces. Thus, to avoid nonspecific interactions, we removed the hydrophobic N-terminal region of synaptotagmin I by cleaving synaptotagmin I at the hypersensitive

Table 1 Ca^{2+} affinities of wild-type and mutant synaptotagmins

	Protein		
Condition	Wild type	R233Q	K236Q
Intrinsic Ca^{2+} affinity in the absence of phospholipids*			
Ca^{2+}-binding site Ca1	54 μM	27 μM	51 μM
Ca^{2+}-binding site Ca2	530 μM	420 μM	530 μM
Ca^{2+}-binding site Ca3	>10 mM	>10 mM	>10 mM
Overall Ca^{2+} affinity in the presence of phospholipid membranes†			
22.5% PS/77.5% PC	40.8 ± 1.9 μM	85.0 ± 7.1 μM	n.d.
30.0% PS/70.0% PC (high density)	11.1 ± 3.0 μM	23.9 ± 4.6 μM	10.6 ± 1.7 μM
30.0% PS/70.0% PC (low density)	12.7 ± 1.3 μM	29.7 ± 4.5 μM	n.d.
45.0% PS/55.0% PC	4.1 ± 0.2 μM	24.5 ± 6.0 μM	n.d.
Overall Ca^{2+} affinity of native synaptotagmin C_2 domains‡			
30.0% PS/70.0% PC	~3–4 μM	~6–8 μM	n.d.

*Dissociation constants were calculated from Ca^{2+} titrations monitored by ^1H–^{15}N HSQC NMR spectra acquired with 150–160 μM recombinant C_2A domains. The Ca^{2+} dependence of the ^{15}N chemical shift of K200 NH resonances from 0.0–0.6 mM total Ca^{2+}, and of the ^1H chemical shift of the S235 NH resonance from 0.5–2.0 mM total Ca^{2+} were used for Ca^{2+}-binding sites Ca1 and Ca2, respectively. Dissociation constants for Ca^{2+}-binding site Ca3 were estimated as it could not be reliably calculated because the binding site was never fully saturated.
† Binding constants represent the EC_{50} obtained from Ca^{2+} titrations of the binding of radiolabelled liposomes to GST–C_2A domain fusion proteins (Fig. 3). Data are means ± s.e.m. from 3–9 independent experiments performed in triplicate with liposomes comprising the indicated phosphatidylserine (PS)/phosphatidylcholine (PC) mixes (n.d. = not determined). For 30% PS/70% PC liposomes, beads were either saturated with the fusion protein (high density), or the fusion protein was diluted in a 1:2 ratio with GST before binding to the beads (low density) to test the effect of protein density on the beads on the apparent Ca^{2+} affinity.
‡ Determined by binding of synaptotagmin cytoplasmic fragments to liposomes using a centrifugation assay (Fig. 5).

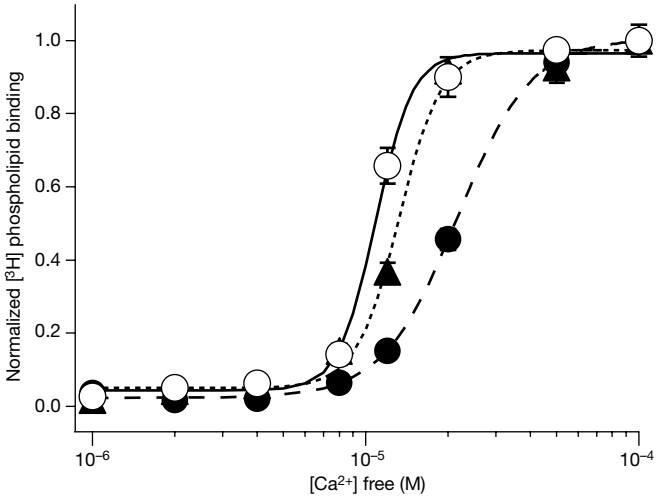

Figure 3 Ca^{2+} dependence of phospholipid binding to wild-type and mutant C_2A domains. Liposomes composed of 30% phosphatidylserine/70% phosphatidylcholine were bound to immobilized GST fusion proteins of wild-type (open circles), R233Q mutant (filled circles) and K236Q mutant (triangles) C_2A domains from synaptotagmin I at the indicated concentrations of free Ca^{2+} clamped with Ca^{2+}/EGTA buffers. Graphs show the means ± s.e.m. of a representative experiment performed in triplicate, and normalized to the binding at saturating Ca^{2+} concentrations; most error bars are not visible because of their small size. EC_{50} values for Ca^{2+}: wild-type, 11 μM; K236Q, 13 μM; R233Q, 21 μM. Results from several independent experiments with different lipid compositions are summarized in Table 1.

proteolytic site between the transmembrane region and the C_2A domain[28,29].

We briefly treated brain homogenates from wild-type and R233Q mutant brains with trypsin, and isolated the cleaved C_2A/C_2B domain fragment in the supernatant after pelleting the membranes. The native C_2A/C_2B domain fragment was used in Ca^{2+}-dependent phospholipid-binding assays by incubating it with liposomes in the presence of defined concentrations of free Ca^{2+}. Liposomes were pelleted, and the amount of C_2A/C_2B domain fragment bound was determined by immunoblotting (Fig. 5a). In parallel, we incubated the C_2A/C_2B domain fragment with glutathione beads containing either glutathione *S*-transferase (GST)–syntaxin or GST alone at different Ca^{2+} concentrations, and measured the amount of bound C_2A/C_2B domain fragment by immunoblotting of the pelleted beads (Fig. 5b).

The data show that the R233Q mutant C_2A/C_2B domain fragment bound phospholipids and syntaxin to a similar extent as did the wild-type C_2A/C_2B domain fragment. However, the R233Q mutant C_2A/C_2B domain fragment exhibited a roughly twofold lower overall Ca^{2+} affinity than that of the wild-type fragment (Fig. 5a), similar to the results obtained with recombinant C_2A domains (Table 1). We observed no consistent difference in syntaxin binding between wild-type and mutant C_2A/C_2B domains, possibly because the more labile, syntaxin-binding assay makes it difficult to detect a twofold shift in Ca^{2+} affinity (Fig. 5b). Notably, the native C_2A/C_2B domain fragment bound to syntaxin at much lower Ca^{2+} concentrations ($< 20\,\mu M$) than previously described for recombinant fragments ($> 200\,\mu M$ Ca^{2+})[19,21]. This result suggests that in native synaptotagmin I, the two C_2 domains cooperate with each other in Ca^{2+} binding and/or are post-translationally modified. Such cooperation and/or modifications could also explain why our previous results suggested that the R233Q mutant C_2A domain is impaired in syntaxin binding[26], whereas the native double C_2-domain fragment is not.

R233Q selectively impairs neurotransmitter release

To test the effects of the R233Q and K236Q mutations on synaptotagmin I function, we cultured hippocampal neurons from newborn knockin mice, and performed electrophysiological recordings in neurons that had formed autapses[9,30–32]. In all experiments, neurons from mutant and wild-type littermates were cultured and analysed simultaneously to control for the variability in synaptic responses between cultures. Neurons from R233Q, K236Q and wild-type knockin mice exhibited robust excitatory postsynaptic currents (EPSCs) in response to action potentials induced by brief depolarizations. However, we observed marked differences between the mutants in the relative EPSC amplitudes during repetitive stimulation (Fig. 6). The EPSC amplitudes of R233Q mutant neurons were smaller than those of wild-type neurons (see below), but displayed large facilitation upon stimulation at 10 Hz, 20 Hz or 50 Hz. Under the same conditions, both wild-type knockin neurons and K236Q knockin neurons exhibited mild synaptic depression (Fig. 6). As a result, the relative synaptic response at the end of a stimulus train was several-fold higher in R233Q mutant neurons than in wild-type neurons and in K236Q mutant neurons,

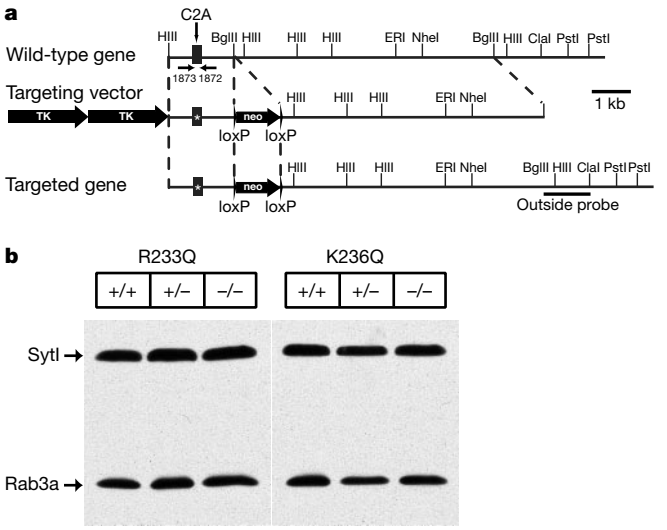

Figure 4 Generation of mice with mutant C_2A domains. **a**, Strategy for creating knockin mice by homologous recombination. A genomic clone containing a single exon from the murine synaptotagmin I gene (top) was used to construct three targeting vectors of the same overall design (middle), with two copies of the thymidine kinase (TK) gene for negative selection and a *neomycin* resistance cassette (neo) for positive selection. In the three vectors, the exon contains the R233Q or the K236Q substitution (asterisk) or is wild type (to generate a precisely matched wild-type control). Homologous recombination replaces the endogenous synaptotagmin I exon with the exon from the targeting vector, and inserts the *neomycin* resistance gene cassette into the intron (bottom). Numbered arrows identify the oligonucleotides (1,872 and 1,873) used for genotyping. The position of the outside probe for detection of homologous recombination by Southern blotting is indicated on the right. Locations of selected restriction sites are shown (HIII = *HindIII*; ERI = *EcoRI*), and the scale is given on the right. **b**, Immunoblots of total brain homogenates (30 μg protein) from wild-type (+/+), heterozygous (+/–) and homozygous (–/–) littermate mice stained with monoclonal antibodies specific for synaptotagmin I and rab3a.

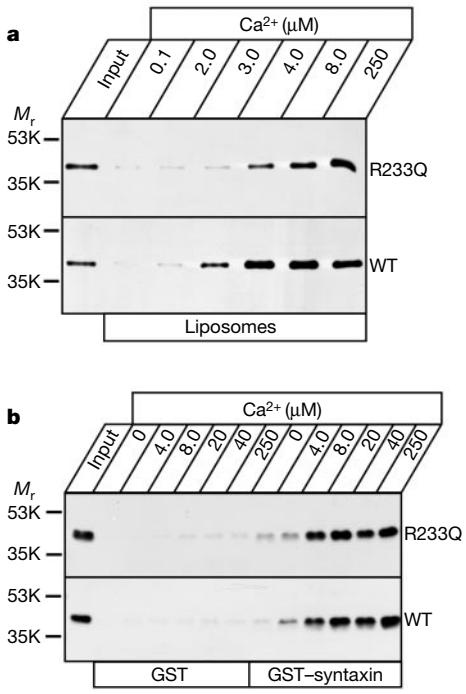

Figure 5 Effect of the R233Q mutation on Ca^{2+}-dependent phosphopholipid and syntaxin binding by native synaptotagmin. **a**, The soluble C_2A/C_2B-domain fragment of synaptotagmin I was obtained from R233Q mutant and wild-type (WT) mice by partial trypsin digestion of synaptotagmin I in brain homogenates. The soluble C_2A/C_2B-domain fragment isolated in the supernatant of centrifuged trypsinized brain homogenates was used for binding experiments with liposomes at the indicated concentrations of free Ca^{2+}. The input and the proteins bound to the liposomes at the various Ca^{2+} concentrations were analysed by immunoblotting using a monoclonal synaptotagmin I antibody. Numbers on the left indicate positions of size markers. **b**, Pull-down experiments of the soluble C_2A/C_2B-domain fragment of synaptotagmin I isolated as described above with GST and with GST–syntaxin (residues 180–264). Experiments were performed with the indicated concentrations of free Ca^{2+} as described in **a**, and bound proteins were visualized by immunoblotting.

suggesting a selective functional effect of the R233Q substitution.

Facilitation during repetitive stimulation is indicative of a reduced release probability[33,34], suggesting that the R233Q mutation changes the efficacy with which Ca^{2+} triggers release during an action potential. The synaptic release probability is the probability with which an action potential stimulates neurotransmitter release at a synapse. It can be measured as the rate of inhibition by an irreversible open-channel blocker of the NMDA (*N*-methyl-D-aspartate) receptor, MK-801 (refs 35, 36). MK-801 only blocks NMDA receptors that have been opened by glutamate, thereby 'knocking out' synapses as they become activated.

To evaluate the effect of the R233Q mutation on synaptic release probability, we measured the rate of inhibition of NMDA-receptor-dependent EPSCs by MK-801. In R233Q mutant and in wild-type neurons, MK-801 caused a multi-exponential decay in the EPSC amplitude, which is consistent with two or more populations of synapses having distinct release probabilities[35,36] (Fig. 7). The decay rate was significantly lower in R233Q mutant neurons than in wild-type neurons, however, showing that the R233Q substitution causes a reduction in synaptic release probability. Assuming that the distribution of release probabilities among synapses is similar between wild-type and R233Q mutant neurons, the decrease in release probability can be quantified as the degree of expansion in the *x* axis of the wild-type curve that is necessary to make it fit to the mutant curve (Fig. 7, inset). This procedure showed that a twofold increase in the scale of the wild-type *x* axis induced a perfect match to the mutant response, suggesting that the R233Q mutation decreased the synaptic release probability twofold.

Vesicular release probability in R233Q mutant mice

A reduction in synaptic release probability could be caused by a decline in the readily releasable pool of synaptic vesicles or by a decrease in the Ca^{2+} triggering of synaptic vesicle exocytosis. In the first case, fewer vesicles would be readily available for release per synapse, but would be normally Ca^{2+} responsive. In the second case, the number of readily releasable vesicles would be unchanged, but the effectiveness of Ca^{2+} influx during an action potential to trigger release would be impaired. To differentiate between these possibilities, we measured consecutively the amplitude of the Ca^{2+}-triggered synaptic response and the size of the readily releasable pool of vesicles in the same neuron (Fig. 8a).

The amplitude of Ca^{2+}-triggered synaptic responses was determined by inducing action potentials with short pulses of depolarization. Evoked responses were then recorded from a large number of mutant and control neurons to obtain representative average EPSC amplitudes. Consistent with the decrease in synaptic release probability (Fig. 7), the amplitude of evoked EPSCs was significantly reduced in R233Q mutant neurons (to ~55 % of the wild-type response) (Fig. 8b). No amplitude reduction was found in K236Q mutant neurons, similar to the lack of a phenotype in the repetitive stimulation paradigm.

To measure the size of the readily releasable pool of synaptic vesicles, we applied hypertonic sucrose (0.5 M), which stimulates exocytosis of the entire readily releasable pool of vesicles by an unknown, Ca^{2+}-independent mechanism[37,38]. In contrast to Ca^{2+}-evoked EPSC amplitudes, no difference in the size of the sucrose

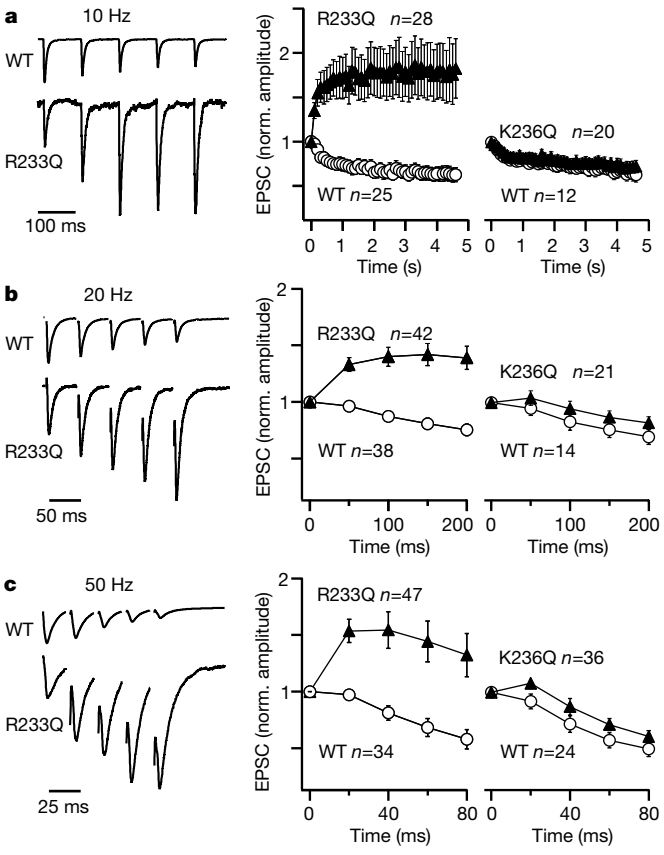

Figure 6 Effect of the R233Q and K236Q mutations on synaptic responses in cultured hippocampal neurons. Evoked synaptic responses were recorded in autapses of cultured hippocampal neurons stimulated at 10 Hz (**a**), 20 Hz (**b**) and 50 Hz (**c**). For each stimulation frequency, representative traces from wild-type (WT) and R233Q mutant neurons are shown on the left, and summary graphs for the respective knockin mutants are shown middle and right for R233Q and K236Q, respectively. Summary graphs compare individual signals from multiple experiments in which mutant and wild-type knockin neurons from littermates were analysed simultaneously to control for culture conditions (means ± s.e.m.). Recordings were made in standard 4 mM Ca^{2+}, 4 mM Mg^{2+} solutions. Vertical calibration bars have been omitted since the currents are normalized to the first response because EPSC amplitudes are lower in the R233Q knockin neurons than in wild-type knockin or K236Q knockin neurons (see Fig. 8).

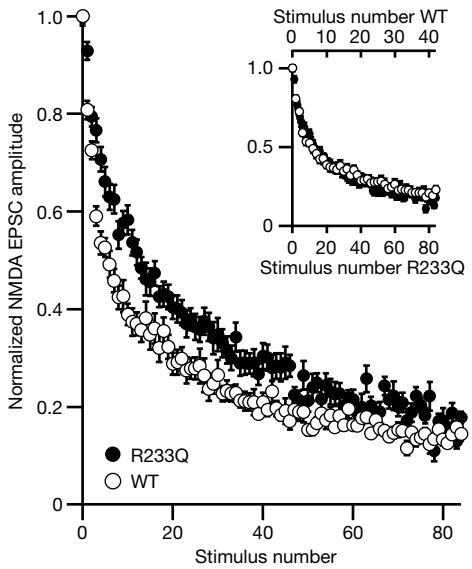

Figure 7 Synaptic release probability in hippocampal neurons from R233Q knockin and wild-type knockin mice. The rate of blockade of excitatory synaptic transmission was recorded as a function of stimulus number in the presence of the irreversible NMDA-receptor inhibitor MK-801 (5 μM). The responses of mutant and wild-type neurons for the same stimulus numbers are compared; the inset shows a plot of the wild-type and mutant signals in which the *x* axis was scaled differentially by a factor of two to match the curves. Responses were recorded in 2.7 mM Ca^{2+}, 0 mM Mg^{2+}, and normalized to the initial synaptic amplitude in MK-801 (~70% of the control NMDA-receptor signal). Data shown are means ± s.e.m. (n = 9 and 16 for wild-type and R233Q mutant neurons, respectively).

response was detected between R233Q mutant neurons and K236Q mutant or wild-type neurons (Fig. 8b). Thus, the R233Q substitution in synaptotagmin I caused a selective decrease in evoked EPSCs that represent Ca^{2+}-triggered fusion, but had no effect on the sucrose response that represents the readily releasable pool. In further support of this conclusion, the frequency and amplitude of spontaneous miniature postsynaptic currents (mEPSCs) were similar in R233Q mutant and wild-type neurons (wild-type, 1.9 ± 0.8 events per second with 13.7 ± 2.5 pA, $n = 5$; R233Q mutant, 2.5 ± 0.8 events per second with 11.5 ± 1.5 pA, $n = 6$).

The vesicular release probability is the probability with which a particular vesicle in the readily releasable pool can be stimulated for exocytosis by Ca^{2+} influx during an action potential[32,38]. This probability can be calculated as the ratio of Ca^{2+}-evoked release to the size of the readily releasable pool. Although in cultured autaptic neurons the sizes of the EPSC amplitudes and of the readily releasable pool vary between cultures, the vesicular release probability of a single neuron is reliably determined when the synaptic responses to action potentials and hypertonic sucrose are recorded in the same neuron (Fig. 8a). For each form of release, the measured charge integral of the postsynaptic currents is the product of the charge of individual mEPSCs (corresponding to release of single vesicles) and the number of released vesicles. Thus, the ratio of the charge integrals of Ca^{2+}-evoked and sucrose-stimulated release measured in a single cell directly corresponds to its vesicular release probability.

When we performed such calculations for the data shown in Fig. 8b, we observed an almost threefold decrease in the vesicular release probability in R233Q mutant neurons compared with that in wild-type knockin neurons that were analysed simultaneously (2.34 ± 0.32%, $n = 44$, versus 6.95 ± 0.85%, $n = 44$; Fig. 8c). No significant difference was detected in the vesicular release probability between K236Q mutant and littermate wild-type neurons (4.6 ± 0.7%, $n = 32$, versus 5.2 ± 0.9%, $n = 23$). Although substantial, the threefold reduction in vesicular release probability in the R233Q mutants is smaller than the tenfold reduction in the release probability observed under the same conditions in synaptotagmin I knockouts (0.6 ± 0.2%, $n = 12$; data not shown). The reduction in vesicular release probability in the R233Q mutants (Fig. 8C) is slightly higher than the reduction in synaptic release probability measured by the rate of MK-801 blockade (Fig. 7), probably because of the distinct Ca^{2+} and Mg^{2+} concentrations that were required for these experiments.

Decreased exocytotic Ca^{2+} sensitivity in R233Q synapses

To obtain a quantitative estimate for the relative Ca^{2+} sensitivity of exocytosis in R233Q mutant and wild-type neurons, we monitored the size of evoked EPSCs as a function of the external Ca^{2+} concentration. Evoked EPSCs were recorded during low-frequency stimulation (0.2 Hz for 30–60 s) at variable Ca^{2+} concentrations (1–12 mM) with a constant Mg^{2+} concentration (1 mM Mg^{2+}) to maximize the release probability, and to allow examination of a large range of Ca^{2+} concentrations. Each test measurement was followed by a control measurement in standard 4 mM Ca^{2+}, 4 mM Mg^{2+} solution to correct for the rundown of synaptic responses during the experiment. We then normalized the response at each test Ca^{2+} concentration to the response at the standard Ca^{2+}/Mg^{2+} concentration obtained immediately afterwards. As the absolute magnitude of the EPSC amplitude is significantly decreased in the R233Q mutant (Fig. 8b), we also normalized the mutant signal to the wild-type signal under standard conditions. In this way, we measured the Ca^{2+} dependence of release independently of the absolute EPSC amplitude.

The resulting Ca^{2+}-response curves reveal two features (Fig. 8d). First, synaptic amplitudes in the R233Q mutant neurons are consistently lower than in wild-type neurons, as expected from the relative depression of release under standard conditions in this mutant (see Fig. 8b). Second, the Ca^{2+}-response curve in the mutant is shifted to the right compared with the wild-type Ca^{2+}-response curve. In the mutant neurons, we could not achieve saturation because increases in extracellular Ca^{2+} beyond 12 mM led to action potential failures and to saturation of Ca^{2+} influx[39]. Nevertheless, high Ca^{2+} concentrations at least partially rescued the mutant phenotype. At the highest Ca^{2+} concentration used (12 mM), the wild-type EPSC amplitude was 1.6 times the control response in standard 4 mM Ca^{2+}, 4 mM Mg^{2+} solution, whereas in R233Q mutant neurons we observed a 2.6-fold increase over the control response (Fig. 8d).

To calculate the apparent affinity for extracellular Ca^{2+}, the dose–response curve was fitted with the Hill function ($I = I_{max} / (1 + (K_d / [Ca^{2+}])^n)$), where I is the recorded synaptic current plotted as normalized amplitude, I_{max} the maximal current, K_d the apparent dissociation constant for extracellular Ca^{2+}, $[Ca^{2+}]$ the extracellular Ca^{2+} concentration, and n the apparent cooperativity. The calculated Ca^{2+} affinity was decreased twofold in R233Q mutant neurons compared to wild-type neurons ($K_d = 3.7 \pm 0.8$ mM versus 1.9 ± 0.2 mM extracellular Ca^{2+}). By contrast, the cooperativity of release, as reflected in the Hill coefficient, was similar (1.7 for wild-type neurons versus 1.6 for R233Q mutant neurons), and the calculated I_{max} of the R233Q neurons was 74% of the wild-type value (1.27 versus 1.72). Note that the external Ca^{2+} affinity and Ca^{2+} cooperativity obviously represent an underestimate of true intracellular Ca^{2+} affinities and cooperativities because they are only indirectly related[39].

Intracellular Ca^{2+} responsiveness in R233Q-mutant synapses

The most plausible explanation for the impaired vesicular release probability in R233Q mutant neurons is that this mutation directly affects the function of the Ca^{2+} sensor for synaptic vesicle exocytosis; however, the impaired vesicular release probability could also be explained by a decrease in Ca^{2+} influx. As synaptotagmin I and syntaxin are known to interact with Ca^{2+} channels[40,41], it is conceivable that the decreased Ca^{2+} responsiveness of synaptic vesicles in the R233Q mutant neurons is due to an inhibition of Ca^{2+} influx. To examine this, we bypassed Ca^{2+}-channel activation by applying the Ca^{2+} ionophore calcimycin. Calcimycin spontaneously inserts into the plasma membrane, and allows Ca^{2+} to flow directly into the neurons. Soon after application of calcimycin, robust Ca^{2+}-induced spontaneous EPSCs were observed in wild-type neurons (Fig. 8e). Application of the same concentration of calcimycin under identical conditions to R233Q mutant neurons led to a delay in the stimulation of EPSCs compared to wild-type neurons (Fig. 8e).

The speed with which a synaptic response is triggered by a Ca^{2+} ionophore will depend on how fast the ionophore inserts into the membrane, how fast Ca^{2+} flows through the ionophore into the terminal, and how much intracellular Ca^{2+} is required in the terminal to trigger release. As the same concentrations of Ca^{2+} ionophore were applied to wild-type and R233Q mutant neurons, the rise in intracellular Ca^{2+} should be identical. Thus, the delayed response in the mutant neurons suggests that higher local Ca^{2+} concentrations in the nerve terminal are necessary to trigger neurotransmitter release from R233Q mutants, consistent with a change in the Ca^{2+} responsiveness of synaptic vesicles downstream of Ca^{2+} channels.

Conclusions

We examined two point mutations in synaptotagmin I, R233Q and K236Q, that neutralize positively charged residues close to the Ca^{2+}-binding sites but have no effect on the three-dimensional structure of synaptotagmin I. R233Q reduces the overall Ca^{2+} affinity of synaptotagmin I, and results in a selective decrease in the Ca^{2+} responsiveness of synaptic vesicle exocytosis. By contrast, K236Q had no effect *in vitro* or *in vivo*. Thus a single-point mutation in synaptotagmin I selectively decreases its overall Ca^{2+} affinity by a

factor of two, and also causes a 2–3-fold decrease in the Ca^{2+} sensitivity of release. The R233Q phenotype is not due to non-specific electrostatic changes because the neighbouring K236Q mutation does not alter the Ca^{2+} affinity of synaptotagmin I or the Ca^{2+} responsiveness of release. The most parsimonious explanation for the effect of the R233Q mutation is that Ca^{2+} binding to synaptotagmin I triggers synaptic vesicle exocytosis; however, this explanation does not imply that synaptotagmin I is the only Ca^{2+} sensor in release as several Ca^{2+} sensors may have to be activated simultaneously to trigger release (for example, several synaptotagmin isoforms).

The similarity of the overall Ca^{2+} affinity of synaptotagmin[14–16] with that of the exocytotic Ca^{2+} sensor in central synapses[22–24], and the parallel shift in these parameters caused by the R233Q mutation, strongly support the role of synaptotagmin I as a Ca^{2+} sensor in release. Nevertheless, alternative explanations could also account for the observed phenotype of the R233Q mutation, although they appear to be less likely than the Ca^{2+}-sensor hypothesis. One alternative explanation is that Ca^{2+} influx is inhibited, leading to a decrease in the apparent Ca^{2+} sensitivity of release. This explanation is unlikely, however, because the Ca^{2+} ionophore experiments revealed that Ca^{2+} triggering is impaired in the R233Q mutant downstream of Ca^{2+} influx.

A second potential explanation for the decrease in apparent Ca^{2+} responsiveness is that Ca^{2+} buffering is increased. This explanation is also improbable because the R233Q mutation causes only a small change in Ca^{2+} binding compared with the large increase in Ca^{2+} buffering required to account for the phenotype. A third potential alternative explanation for the R233Q phenotype is that R233 mediates binding of an unidentified protein to synaptotagmin I which is the 'true' Ca^{2+} sensor in release instead of synaptotagmin. To be the true Ca^{2+} sensor, however, the unidentified synaptotagmin I ligand—possibly the SNARE complex—would itself have to bind Ca^{2+} but interact equally well with Ca^{2+}-bound and Ca^{2+}-free synaptotagmin I (otherwise synaptotagmin I would, after all, still be a Ca^{2+} sensor in release). These conditions make this explanation also rather unlikely, especially in view of the role of R233 in Ca^{2+} binding to synaptotagmin I.

What is the mechanism of action of synaptotagmin I as a Ca^{2+} sensor/transducer in release? In proteins such as perforin, PKC and phospholipase C, phospholipid binding to C_2 domains mediates the Ca^{2+}-dependent regulation[42–45]. By analogy, it seems plausible that binding of the C_2 domains of synaptotagmin I to phospholipid membranes is integral to its function. Synaptotagmin I is present on docked vesicles at the active zone close to the plasma membrane, and thus has ready access to phospholipid membranes. In addition, the interaction of synaptotagmin I with syntaxin provides an attractive mechanism of action because of the fundamental role of

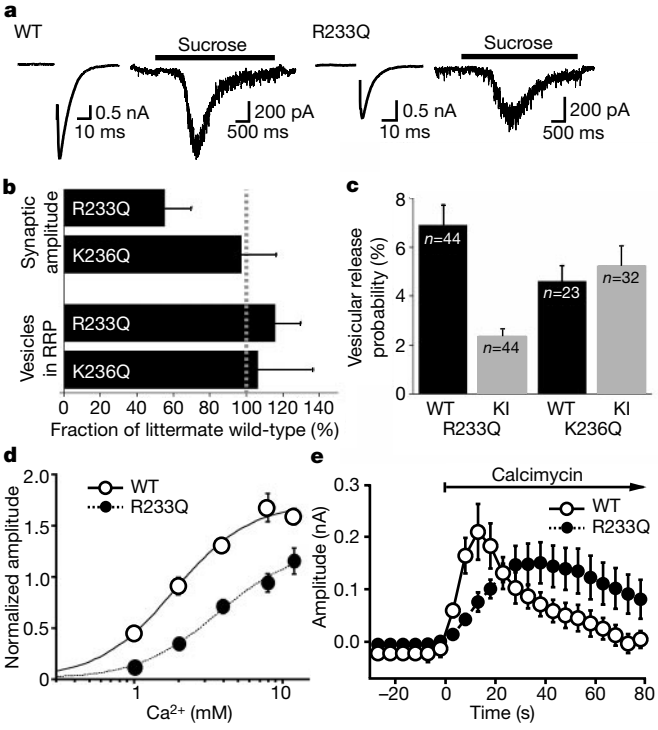

Figure 8 Pool sizes and Ca^{2+} responsiveness of synaptic vesicles in wild-type, R233Q and K236Q mutant synapses. **a**, Typical synaptic responses evoked by action potentials or application of hypertonic sucrose in neurons from wild-type and R233Q knockin mice. Action potentials were induced by short somatic depolarization (from −75 mV to 0 mV for 2 ms), and the readily releasable pool of vesicles was stimulated from the same cell by hypertonic sucrose (0.5 M for 3 s). Capacitative and somatic currents are blanked for display purposes. **b**, Quantitative analysis of the synaptic EPSC amplitudes and the size of the readily releasable pool of R233Q and K236Q knockin neurons compared with wild type. Mean amplitudes and pool sizes recorded in mutant knockin neurons were normalized to wild-type knockin littermate controls; responses are expressed as per cent of wild-type controls (100% = dotted line; *n* is the same as in **c**). **c**, Mean vesicular release probability expressed as a per cent of the readily releasable pool. R233Q and K236Q knockin neurons were analysed simultaneously with wild-type knockin control neurons from littermates, and are shown in comparison with these controls to correct for culture-dependent variability. Vesicular release probability was obtained from recordings in which evoked EPSCs and the readily releasable pool were measured in the same cells, and is calculated as the ratio of the evoked EPSC charge integral to the sucrose-stimulated charge integral. **d**, Ca^{2+} dependence of release from wild-type knockin (WT) and R233Q knockin synapses. Synaptic responses to brief depolarizations were recorded at the indicated concentrations of Ca^{2+} in the presence of 1 mM Mg^{2+}. The same neurons were examined consecutively for all Ca^{2+} concentrations, with control measurements in standard 4 mM Ca^{2+}, 4 mM Mg^{2+} solutions after each test measurement to correct for the rundown of responses during recordings; responses are additionally normalized for the absolute EPSC amplitudes. Data shown are means ± s.e.m. (n = 6–16 and 8–18 cells for wild-type and R233Q knockin neurons, respectively). **e**, Spontaneous synaptic EPSCs evoked by the Ca^{2+} ionophore calcimycin in wild-type (WT) and R233Q knockin neurons. Calcimycin was applied at time 0 after stable baseline recordings for 100 s. Data shown are means ± s.e.m. (n = 9 and 12 cells for wild-type and R233Q knockin neurons, respectively). All recordings except for those in **d** were made in standard 4 mM Ca^{2+}, 4 mM Mg^{2+} solutions.

syntaxin in synaptic vesicle fusion[46]. The absolute Ca^{2+} dependence and the markedly lower Ca^{2+} requirement for syntaxin binding to native synaptotagmin (as opposed to recombinant synaptotagmin[19,21]) fit well with the role of an exocytotic Ca^{2+} sensor[22–24]. Although we were unable to detect a change in syntaxin binding in the R233Q mutant, it is possible that Ca^{2+}-dependent phospholipid and syntaxin binding to synaptotagmin I cooperate in Ca^{2+} triggering of exocytosis. This might occur together with additional Ca^{2+}-dependent activities of the C_2 domains, such as the Ca^{2+}-dependent multimerization of synaptotagmin I (refs 47, 48). Independent of the precise mechanism of action of synaptotagmin I, however, our data show that synaptotagmin I is a direct component of the Ca^{2+} sensor in synchronous release where alterations in its overall Ca^{2+} affinity translate into equivalent changes in the Ca^{2+} sensitivity of neurotransmitter release. □

Methods

Ca^{2+}-binding studies of C_2A domains

$^1H-^{15}N$ HSQC spectra were acquired at 25 °C in a Varian INOVA500 NMR spectrometer (spectral widths = 7,600 and 1,163 Hz in the ^1H and ^{15}N dimensions, respectively) using uniformly ^{15}N-labelled C_2A domains[11–13,49]. Initial Ca^{2+} titrations were recorded at 150–160 μM protein concentrations using $^1H-^{15}N$ HSQC spectra (1 h total acquisition time) with successive additions of 0, 0.05, 0.1, 0.15, 0.2, 0.25, 0.3, 0.375, 0.45, 0.525, 0.6, 0.675, 0.75, 1, 1.2, 2, 5, 10, 20, 30 and 40 mM Ca^{2+}. Additional Ca^{2+} titrations of 18–20 μM wild-type and R233Q mutant C_2A domains were obtained with $^1H-^{15}N$ HSQC spectra (12 h total acquisition time) recorded after successive additions of 0, 10, 20, 40, 60, 80, 100, 140, 180 and 220 μM Ca^{2+} (wild-type) and 0, 5, 10, 20, 40, 60, 80 and 100 μM Ca^{2+} (mutant). The Ca^{2+} affinities of the different sites were calculated by curve fitting the Ca^{2+} dependence of selected chemical shifts to standard protein–ligand equilibrium equations using Sigma Plot.

Phospholipid-binding studies of C_2A domains

^3H-labelled liposomes containing the indicated concentrations of PS and PC were prepared by sonication, and used in phospholipid-binding assays with immobilized GST or GST fusion proteins of the C_2A domains[14,15]. Binding assays were carried out with identical amounts of liposomes, protein and glutathione–agarose using Ca^{2+}/EGTA buffers calculated with EqCal (Biosoft, Cambridge, UK). To test the effect on the apparent Ca^{2+} affinity of the density of the C_2A domain fusion protein on the beads, beads were loaded with a 2:1 mixture of GST to the GST–C_2A domain fusion protein, and the binding assays were performed with these diluted C_2A domains.

Phospholipid and syntaxin binding

Post-nuclear supernatants from mouse brains in 20 mM HEPES-NaOH pH 7.2, 0.1 g l^{-1} PMSF were diluted to 8 g protein per l and digested with 0.008% trypsin for 30 min at 37 °C. Afterwards, 0.1 g l^{-1} soybean trypsin inhibitor, 1% goat serum, and 1 mM PMSF were added, samples were centrifuged at 300,000*g* for 4 h at 4 °C, and the supernatants were re-centrifuged for an additional 30 min. Aliquots (1.1 ml) of the supernatants and of 2.4× Ca^{2+}/EGTA-buffers in 80 mM HEPES-NaOH pH 7.2, 0.2 M NaCl were mixed. One millilitre of each sample was distributed into two tubes, 0.2 ml of 0.5 g l^{-1} liposomes were added in 50 mM HEPES-NaOH pH 7.2, 0.1 M NaCl, and samples were incubated at 36 °C for 15 min under agitation. Liposomes were pelleted by centrifugation (100,000*g* for 30 min), washed once in the appropriate Ca^{2+}/EGTA buffer, and analysed by SDS–PAGE and immunoblotting using Cl41.1 synaptotagmin I monoclonal antibody.

For GST–syntaxin binding assays, trypsinized brain extracts were aliquoted with Ca^{2+}/EGTA buffers as described above with 1% Triton X-100 in the final solutions. Agarose beads with GST–syntaxin 180–264 or GST alone (1–2 g protein per l glutathione agarose) were preblocked in 20 mM HEPES-NaOH pH 7.2, 1% BSA for 30–90 min at 4 °C, pelleted, and 1.2 ml of trypsinized brain extract in Ca^{2+}/EGTA buffer was added. Samples were incubated overnight at 4 °C on a rotator, pelleted, washed three times with the appropriate incubation buffers, and pelleted again. Bound proteins were analysed by SDS–PAGE and immunoblotting as described above.

Generation of knockin mutant mice

We used a genomic λ-clone containing a single exon with residues 214–269 of murine synaptotagmin I to construct three similar targeting vectors with either wild-type or R233Q and K236Q mutant exon sequences (Fig. 4). Vectors were electroporated into embryonic stem cells (E14 cells, a gift from K. von Figura, Göttingen), colonies were selected with G418 and gancyclovir[27], and double-resistant colonies were analysed for homologous recombination by Southern blotting with an outside probe. Clones containing homologously recombined genes were expanded, confirmed by PCR, and used to generate mice by blastocyst injection. All three resulting mouse lines had the *neomycin* resistance gene in the intron next to the exon which was either wild-type or carried the R233Q or K236Q mutation. To ensure that all analysis was performed on precisely matched controls, all mutant mice were maintained as double heterozygotes of wild-type/mutant knockin on a mixed SV129/Black 6 background, and all analyses were performed on littermates derived from matings between double heterozygotes. Mice of various genotypes and wild-type control mice were studied by immunoblotting for synaptic proteins as described[27].

Electrophysiological analyses of hippocampal neurons

Individual cultures of hippocampal neurons from all mice in a litter from double-heterozygous mutant/wild-type knockin mice were prepared at P0 or P1 on microislands of glia cells (pre-plated in 10% fetal bovine serum) under conditions favouring formation of autapses, and used for experiments after 10–20 d in culture[30–32]. Before seeding neurons in a density of 500 per cm^2, the medium was exchanged to neurobasal medium A (Gibco) with supplement B27 (Gibco). Only dots containing single neurons were used. Only excitatory EPSCs were analysed since too few measurements were obtained from inhibitory GABAergic. The extracellular medium for the cultures contained (in mM): NaCl 140, KCl 2.4, HEPES 10, glucose 10, $CaCl_2$ 4, $MgCl_2$ 4; pH 7.3; 300 mOsm. For the measurements of mEPSCs, tetrodotoxin (200 nM) was added. NMDA EPSCs were measured in the presence of external 2.7 mM Ca^{2+} and 10 μM glycine but without Mg^{2+}. Synaptic transmission was recorded in the whole-cell configuration under voltage-clamp using 1–2 ms depolarizations from −75 mV to 0 mV to induce action potentials. Hypertonic sucrose solutions contained 0.5 M sucrose in addition to the regular external solution. Patch pipette solutions included (in mM): K-gluconate 125, NaCl 10, $MgCl_2$ 4.6, ATP-Na_2 4, creatine phosphate 15, phosphocreatine kinase (20 U ml^{-1}), EGTA 1; buffer pH 7.3; 300 mOsm. Chemicals were purchased from Sigma, except for MK-801 (Tocris).

Received 9 October; accepted 12 December 2000.

1. Katz, B. *The Release of Neural Transmitter Substances* (Liverpool Univ. Press, Liverpool, 1969).
2. Borst, J. G. & Sakmann, B. Calcium influx and transmitter release in a fast CNS synapse. *Nature* **383,** 431–434 (1996).
3. Sabatini, B. L. & Regehr, W. G. Timing of synaptic transmission. *Annu. Rev. Physiol.* **61,** 521–542 (1999).
4. Bennett, M. R. The concept of a calcium sensor in transmitter release. *Prog. Neurobiol.* **59,** 243–277 (1999).
5. Burgoyne, R. D. & Morgan, A. Calcium sensors in regulated exocytosis. *Cell Calcium* **24,** 367–376 (1998).
6. Kelly, R. B. Neural transmission. Synaptotagmin is just a calcium sensor. *Curr. Biol.* **5,** 257–259 (1995).
7. von Gersdorff, H. & Matthews, G. Electrophysiology of synaptic vesicle cycling. *Annu. Rev. Physiol.* **61,** 725–752 (1999).
8. Perin, M. S., Fried, V. A., Mignery, G. A., Jahn, R. & Südhof, T. C. Phospholipid binding by a synaptic vesicle protein homologous to the regulatory region of protein kinase C. *Nature* **345,** 260–263 (1990).
9. Geppert, M. *et al.* Synaptotagmin I: A major Ca^{2+} sensor for transmitter release at a central synapse. *Cell* **79,** 717–727 (1994).
10. Sutton, R. B., Davletov, B. A., Berghuis, A. M., Südhof, T. C. & Sprang, S. R. Structure of the first C_2-domain of synaptotagmin I: a novel Ca^{2+}/phospholipid-binding fold. *Cell* **80,** 929–938 (1995).
11. Shao, X., Fernandez, I., Südhof, T. C. & Rizo, J. Solution structures of the Ca^{2+}-free and Ca^{2+}-bound C_2A-domain of synaptotagmin I: does Ca^{2+} induce a conformational change? *Biochemistry* **37,** 16106–16115 (1998).
12. Ubach, J., Zhang, X., Shao, X., Südhof, T. C. & Rizo, J. Ca^{2+} binding to synaptotagmin: how many Ca^{2+} ions bind to the tip of a C_2-domain? *EMBO J.* **17,** 3921–3930 (1998).
13. Shao, X., Davletov, B. A., Sutton, R. B., Südhof, T. C. & Rizo, J. A bipartite Ca^{2+}-binding motif in C_2-domains of synaptotagmin and protein kinase C. *Science* **273,** 248–251 (1996).
14. Davletov, B. & Südhof, T. C. A single C_2-domain from synaptotagmin I is sufficient for high affinity Ca^{2+}/phospholipid-binding. *J. Biol. Chem.* **268,** 26386–26390 (1993).
15. Zhang, X., Rizo, J. & Südhof, T. C. Mechanism of phospholipid binding by the C_2A-domain of synaptotagmin I. *Biochemistry* **36,** 12395–12403 (1998).
16. Brose, N., Petrenko, A. G., Südhof, T. C. & Jahn, R. Synaptotagmin: A Ca^{2+} sensor on the synaptic vesicle surface. *Science* **256,** 1021–1025 (1992).
17. Mosior, M. & Epand, R. M. Characterization of the calcium-binding site that regulates association of protein kinase C with phospholipid bilayers. *J. Biol. Chem.* **269,** 13798–13805 (1994).
18. Verdaguer, N., Corbalan-Garcia, S., Ochoa, W. F., Fita, I. & Gomez-Fernandez, J. C. Ca^{2+} bridges the C_2 membrane-binding domain of protein kinase Cα directly to phosphatidylserine. *EMBO J.* **18,** 6329–6338 (2000).
19. Li, C. *et al.* Ca^{2+}-dependent and Ca^{2+}-independent activities of neural and nonneural synaptotagmins. *Nature* **375,** 594–599 (1995).
20. Chapman, E. R., Hanson, P. I., An, S. & Jahn, R. Ca^{2+} regulates the interaction between synaptotagmin and syntaxin 1. *J. Biol. Chem.* **270,** 23667–23771 (1995).
21. Kee, Y., Scheller & R. H. Localization of synaptotagmin-binding domains on syntaxin. *J. Neurosci.* **16,** 1975–1981 (1996).
22. Lagnado, L., Gomis, A. & Job, C. Continuous vesicle cycling in the synaptic terminal of retinal bipolar cells. *Neuron* **17,** 957–967 (1996).
23. Schneggenburger, R. & Neher, E. Intracellular calcium dependence of transmitter release rates at a fast central synapse. *Nature* **406,** 889–893 (2000).
24. Bollmann, J. H., Sakmann, B. & Borst, J. G. Calcium sensitivity of glutamate release in a calyx-type terminal. *Science* **289,** 953–957 (2000).
25. Garcia, R. A., Forde, C. E. & Godwin, H. A. Calcium triggers an intramolecular association of the C_2-domains in synaptotagmin. *Proc. Natl Acad. Sci. USA* **97,** 5883–5888 (2000).
26. Shao, X. *et al.* Synaptotagmin–syntaxin interaction: the C_2-domain as a Ca^{2+}-dependent electrostatic switch. *Neuron* **18,** 133–142 (1997).
27. Rosahl, T. W. *et al.* Essential functions of synapsins I and II in synaptic vesicle regulation. *Nature* **375,** 488–493 (1995).
28. Perin, M. S., Brose, N., Jahn, R. & Südhof, T. C. Domain structure of synaptotagmin. *J. Biol. Chem.* **266,** 623–629 (1991).
29. Tugal, H. B., van Leeuwen, F., Apps, D. K., Haywood, J. & Phillips, J. H. Glycosylation and transmembrane topography of bovine chromaffin granule p65. *Biochem. J.* **279,** 699–703 (1991).
30. Bekkers, J. M. & Stevens, C. F. Excitatory and inhibitory autaptic currents in isolated hippocampal neurons maintained in cell culture. *Proc. Natl Acad. Sci. USA* **88,** 7834–7838 (1991).

31. Gomperts, S. N., Rao, A., Craig, A. M., Malenka, R. C. & Nicoll, R. A. Postsynaptically silent synapses in single neuron cultures. *Neuron* **21,** 443–451 (1998).
32. Augustin, I., Rosenmund, C., Südhof, T. C. & Brose, N. Munc-13 is essential for fusion competence of glutamatergic synaptic vesicles. *Nature* **400,** 457–461 (1999).
33. Zucker, R. S. Short-term synaptic plasticity. *Annu. Rev. Neurosci.* **12,** 13–31 (1989).
34. Thomson, A. M. Facilitation, augmentation and potentiation at central synapses. *Trends Neurosci.* **23,** 305–312 (2000).
35. Rosenmund, C., Clements, J. D. & Westbrook, G. L. Nonuniform probability of glutamate release at a hippocampal synapse. *Science* **262,** 754–757 (1993).
36. Hessler, N. A., Shirke, A. M. & Malinow, R. The probability of transmitter release at a mammalian central synapse. *Nature* **366,** 569–572 (1993).
37. Rosenmund, C. & Stevens, C. F. Definition of the readily releasable pool of vesicles at hippocampal synapses. *Neuron* **16,** 1197–1207 (1996).
38. Fatt, P. & Katz, B. Spontaneous subthreshold activity at motor nerve endings. *J. Physiol. (Lond.)* **117,** 109–128 (1952).
39. Mintz, I. M., Sabatini, B. L. & Regehr, W. G. Calcium control of transmitter release at a cerebellar synapse. *Neuron* **15,** 675–688 (1995).
40. Catterall, W. A. Interactions of presynaptic Ca^{2+}-channels and SNARE proteins in neurotransmitter release. *Ann. N. Y. Acad. Sci.* **868,** 144–159 (1999).
41. Seagar, M. *et al.* Interactions between proteins implicated in exocytosis and voltage-gated calcium channels. *Phil. Trans. R. Soc. Lond. B* **354,** 289–297 (1999).
42. Uellner, R. *et al.* Perforin is activated by a proteolytic cleavage during biosynthesis which reveals a phospholipid-binding C_2-domain. *EMBO J.* **16,** 7287–7296 (1997).
43. Edwards, A. S. & Newton, A. C. Regulation of protein kinase CβII by its C_2-domain. *Biochemistry* **36,** 15615–15623 (1997).
44. Nalefski, E. A. & Falke, J. J. Location of the membrane-docking face on the Ca^{2+}-activated C_2-domain of cytosolic phospholipase A2. *Biochem.* **37,** 17642–17650 (1998).
45. Williams, R. L. & Katan, M. Structural views of phosphoinositide-specific phospholipase C: signalling the way ahead. *Structure* **4,** 1387–1394 (1996).
46. Blasi, J. *et al.* Botulinum neurotoxin C1 blocks neurotransmitter release by means of cleaving HPC-1/syntaxin. *EMBO J.* **12,** 4821–4828 (1993).
47. Sugita, S., Hata, Y. & Südhof, T. C. Distinct Ca^{2+}-dependent properties of the first and second C_2-domains of synaptotagmin I. *J. Biol. Chem.* **271,** 1262–1265 (1996).
48. Chapman, E. R., An, S., Edwardson, J. M. & Jahn, R. A novel function for the second C_2-domain of synaptotagmin. Ca^{2+}-triggered dimerization. *J. Biol. Chem.* **271,** 5844–5849 (1996).
49. Zhang, O., Kay, L. E., Olivier, J. P. & Forman-Kay, J. Backbone ^{1}H and ^{15}N resonance assignments of N-terminal SH3 domain of drk in folded and unfolded states using enhanced-sensitivity pulsed field gradient NMR techniques. *J. Biomol. NMR* **4,** 845–858 (1994).

Supplementary information is available on *Nature*'s World-Wide Web site (http://www.nature.com) or as paper copy from the London editorial office of *Nature*.

Acknowledgements

We thank I. Herfort, I. Leznicki and A. Roth for technical assistance; H. Riedesel, J. Krause, S. Röcklin and the ARC in Dallas for help with mouse husbandry; and E. Neher, G. Alvarez de Toledo, J. López-Barneo and R. Jahn for advice. This study was supported by grants from the NIH to J.R., a grant from the Deutsche Forschungsgemeinschaft to C.R., Heisenberg Fellowships from the Deutsche Forschungsgemeinschaft to N.B. and C.R., a grant from the Perot Family Foundation to T.C.S., and postdoctoral fellowships from the Spanish Ministry of Education and the Fulbright Commission to R.F.C., and from the Deutsche Forschungsgemeinschaft to S.H.G.

Correspondence and requests for materials should be addressed to T.C.S. (e-mail: Thomas.Sudhof@UTSouthwestern.edu).